

AttributionScanner: A Visual Analytics System for Metadata-Free Data-Slicing Based Model Validation

Xiwei Xuan, Jorge Piazzentin Ono, Liang Gou, Kwan-Liu Ma, and Liu Ren

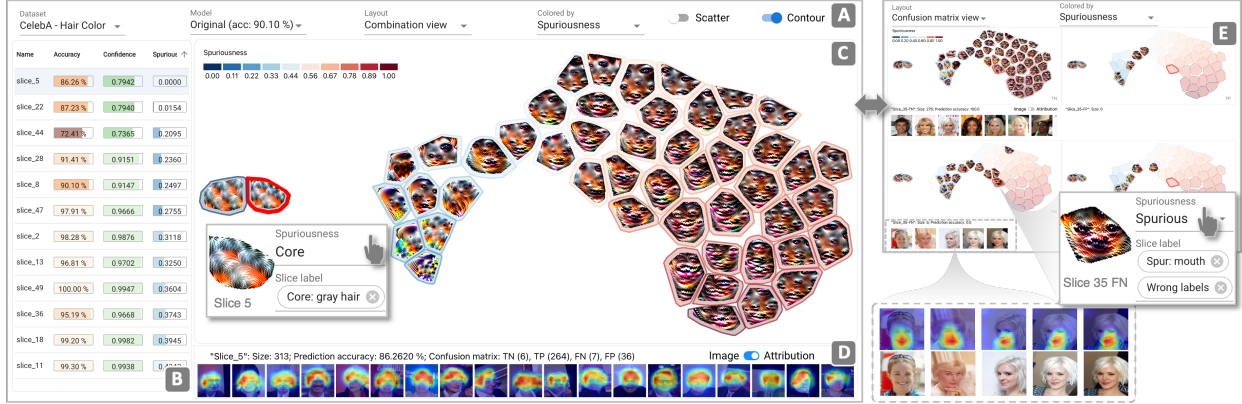


Fig. 1: *AttributionScanner* applied to the model validation of a hair color classifier trained on the CelebA image dataset [22]. **A** System Menu, enabling the selection of dataset, model, and visualization options (Layout, Confusion Matrix, Scatter Plot/*Data Slice Mosaic*, and Contour Visibility). **B** Slice Table, showing the data slices and slice metrics. **C** *Data Slice Mosaic*, showing a visual overview of all data slices, which can also be displayed in the cells of a confusion matrix view (**E**). **D** Slice Detail View, showing individual images or Attribution Heatmaps belonging to a selected data slice.

Abstract—Data slice-finding is an emerging technique for evaluating machine learning models. It works by identifying subgroups within a specified dataset that exhibit poor performance, often defined by distinct feature sets or meta-information. However, in the context of unstructured image data, data slice-finding poses two notable challenges: it requires additional metadata—a laborious and costly requirement, and also demands non-trivial efforts for interpreting the root causes of the underperformance within data slices. To address these challenges, we introduce *AttributionScanner*, an innovative human-in-the-loop Visual Analytics (VA) system, designed for data-slicing-based machine learning (ML) model validation. Our approach excels in identifying interpretable data slices, employing explainable features extracted through the lens of Explainable AI (XAI) techniques, and removing the necessity for additional metadata of textual annotations or cross-model embeddings. *AttributionScanner* demonstrates proficiency in pinpointing critical model issues, including spurious correlations and mislabeled data. Our novel VA interface visually summarizes data slices, enabling users to gather insights into model behavior patterns effortlessly. Furthermore, our framework closes the ML Development Cycle by empowering domain experts to address model issues by using a cutting-edge neural network regularization technique. The efficacy of *AttributionScanner* is underscored through two prototype use cases, elucidating its substantial effectiveness in model validation for vision-centric tasks. Our approach paves the way for ML researchers and practitioners to drive interpretable model validation in a data-efficient way, ultimately leading to more reliable and accurate models.

Index Terms—Model validation, visual analytics, data slicing, model evaluation, data-centric AI, human-assisted AI, human-in-the-loop.

1 INTRODUCTION

As Machine Learning (ML) technologies continue to permeate various domains, the importance of ML model validation has grown significantly. More specifically, understanding the circumstances and reasons behind a model’s success or failure is crucial in promoting greater model transparency, accountability, and accuracy. A powerful strategy supporting this effort is Data Slice-Finding [29, 47]. These methods aim to identify specific instances or data subgroups, referred to as data-

slices, where a model’s performance falls short compared to overall cases. These data slices are commonly defined by tabular features or meta-information, which represent contextual details about the samples, such as their collection methods, feature descriptions, and other relevant information. The problematic data slices may arise from under-represented samples or biased datasets, for example [47].

Upon the identification of these problematic data slices, there mainly exist two remedial strategies for model developers to enhance the models. Firstly, they could focus on training or fine-tuning the models on these identified subgroups to bolster the model’s overall reliability [11]. Alternatively, employing eXplainable Artificial Intelligence (XAI) [13] techniques could reveal potential causal factors adversely impacting the model, thus enabling a tactical manipulation of model’s internal parameters to improve the performance [34].

However, despite the promising benefits of data slice-finding and XAI techniques in explaining problematic data slices, several hurdles remain unaddressed for a thorough model validation.

Challenges of Data Slice-Finding. Slice-finding techniques operate by grouping the data into subsets sharing a mutual characteristic [7, 9,

- Xiwei Xuan and Kwan-Liu Ma are with UC Davis. Xiwei Xuan is an intern at Bosch Research. E-mails: {xwxuan, klma}@ucdavis.edu.
- Jorge P. Ono, Liang Gou, and Liu Ren are with Robert Bosch Research and Technology Center, USA - Bosch Center for Artificial Intelligence. E-mails: {jorge.piazzentinono, liang.gou, liu.ren}@us.bosch.com.

Manuscript received xx xxx. 201x; accepted xx xxx. 201x. Date of Publication xx xxx. 201x; date of current version xx xxx. 201x. For information on obtaining reprints of this article, please send e-mail to: reprints@ieee.org.
Digital Object Identifier: xx.xxx/TVCG.201x.xxxxxxx

11, 30, 35, 40]. To generate human-interpretable data subgroups, state-of-the-art slice-finding methods demand extensive meta-information associated with each data instance. While many works use existing tabular data descriptors to compute the slices [7, 30, 35], others apply multi-modal pre-trained vision-language models to generate descriptive information for slice-finding [11]. These approaches, however, pose two main challenges. The first is the significant human effort required to manually collect additional data descriptions. The second challenge arises because vision-language models are trained with general purpose data, which can contain biased knowledge about a domain-specific scenario. In situations where neither metadata nor suitable pre-trained models are available, generating interpretable data subgroups becomes a labor-intensive and challenging task. This process requires users to manually examine a large number of data samples individually in order to hypothesize, understand, and validate the details of each slice. [9, 40].

Challenges of XAI for Vision Models. Given troublesome data slices, it also requires non-trivial efforts to uncover the root causes of a model’s failure on these cases. Even with the advanced human-friendly XAI techniques, there still exist a few challenges. Predominantly, most model explanation methods are instance-based, conducting a thorough examination of all instances to derive conclusions based on a big picture is practically unfeasible [27, 33, 37, 48]. Moreover, the insights we can obtain from existing methods are often not actionable, which means what the common failure patterns are and how to address them remain vague and demands further study.

Our approach. We present *AttributionScanner*, a Visual Analytics (VA) system designed to address the above challenges: it generates interpretable data slices and provides users with sufficient guidance for validating vision models without any meta-information. Our innovative workflow employs attribution-based explanation techniques to create interpretable feature representations for slice finding, enabling unstructured image data to be sliced based on the model’s behavior patterns. Moreover, we explain the discriminating features of each data slice via visual summaries, called *Data Slice Mosaic*, to guide users in explaining model’s behaviors and detecting potential issues, thus facilitating model validation. Additionally, *AttributionScanner* integrates a human-in-the-loop approach to rank and annotate the problematic data slices based on common error types such as mislabeled samples and spurious correlations. Our approach enables users to apply these annotated slices to enhance the model, by correcting the identified errors on either the model or data side. Our main contributions include:

1. *AttributionScanner*, a novel framework and VA system employing data slice-finding to validate vision models. Unlike existing methods, *AttributionScanner* removes the need for prior knowledge, like meta-information or cross-modal embeddings, to generate meaningful data slices for model validation. Our novel attribution representation space enables explainable data slicing, supporting the quick detection of data and model problems, such as spurious correlations and mislabeled data.
2. *Data Slice Mosaic*, an innovative slice summarization method that visually encapsulates the significant model behavior pattern of different slices. Our method allows users to quickly understand and validate the contents of data slices, reducing the effort in conventional approaches of examining a large volume of individual data samples.
3. A novel workflow for optimizing models based on insights generated by *AttributionScanner*. This workflow enables users to swiftly detect, understand, and fix model issues related to spurious correlations and mislabeled data.
4. Finally, we underscore the efficacy of *AttributionScanner* through two use cases that highlight its ability to identify and mitigate data slice problems in machine learning vision models.

This paper is structured as follows: in Sec. 2, we review related work on Data Slice-Finding and XAI that is relevant to our work. Sec. 3 outlines the methodology and system design of *AttributionScanner*. In Sec. 4, we illustrate two use cases showcasing how *AttributionScanner* can be utilized for vision model validation. An evaluation of our

system and experts’ feedback are discussed in Sec. 5. Lastly, we present our future work and conclusions in Sec. 7.

2 RELATED WORK

Our method, *AttributionScanner*, leverages insights from both Data Slice-Finding and XAI techniques for Neural Networks to pinpoint problematic data slices in vision-based models. This provides a brief overview of the relevant literature on these two topics.

2.1 Data Slice-Finding

Data Slice-Finding is a technique used to identify data subsets where ML models underperform. These subsets are usually defined by a combination of feature-value pairs extracted from tabular metadata. However, the exponential search space associated with this task makes it a challenging problem. To overcome this challenge, heuristics have been presented to approximate the solution. Barash et al. [3] introduced a Combinatorial Modeling-based approach that enumerates the space of value combinations in tabular data up to a set number of parameters. Similarly, Slice Finder [7] uses a decision tree heuristic to identify interpretable data slices that can be described by decision tree rules. Despite the advantages of heuristics, they may miss important data slices. Therefore, new techniques have been developed to enable the exhaustive search of data slices using novel formulations and parallel architectures. DivExplorer [29] employs frequent pattern mining to enumerate all candidate slices in the data and identify the most relevant ones based on frequency or metric divergence. In contrast, SliceLine [35] introduces a vectorized formulation for Slice Finding, which can be easily deployed in parallel devices.

The aforementioned methods necessitate structured metadata to segment datasets into meaningful subgroups, a requirement challenging to meet, especially in domains with large volumes of image or text data where detailed meta-information may be scarce. To address this, a prevalent approach involves encoding data samples into the model’s latent space, followed by clustering to group the data and pinpoint problematic slices. For instance, GEORGE [40] employs over-clustering alongside Group Distributionally Robust Optimization [36] to automatically detect and rectify distribution shift-induced errors. Spotlight [9] adopts a soft-clustering strategy, evaluating performance metrics per cluster and pinpointing clusters with the highest performance drops as data slices for user review. Similarly, UDIS [18] implements hierarchical clustering and further GradCAM [37] visual explanations for data slice examination. VisCUIT [20] allows a deeper exploration of the UDIS data slices by enabling slice comparison and the exploration of neuron activations per slice. Although these methods can support the identification of problematic slices, users have to delve into individual samples to understand model failure reasons. Domino [11] mitigates this by utilizing a pre-trained vision-language model for generating textual descriptions of slices, encoding images into model embedding, and clustering them based on shared visual attributes. However, this method’s reliance on pre-trained models for slice identification and explanation can backfire if there’s a significant domain mismatch between the dataset being evaluated and the pre-trained model, possibly yielding unmeaningful slices. In Sec. 3, we introduce a methodology capable of producing explainable slices independently of such pre-trained models.

Visualization has also proven effective in identifying problematic subgroups of data. Kahng et al. introduced a data cube analysis method [17], in which the performance of models was assessed on data slices defined by all pairwise combinations of data features. Meanwhile, FairVis [5] enables users to manually slice and inspect data slices based on domain knowledge to identify potential model biases. Similarly, Errudite [44] came up with a domain-specific language to allow the data slicing of textual documents based on linguistic features and model testing under specific conditions. Although manually slicing the data is useful for model analysis, this approach is not scalable since there could be an exponential number of slices to evaluate. To address this issue, SliceTeller [47] combined an automatic slice-finding algorithm with a visual analytics tool to allow the analysis and iterative refinement of models. However, it still required structured metadata in order to produce meaningful data slices. In Sec. 3, we present a visual

analytics tool that requires no metadata or prior information to produce meaningful data slices.

2.2 XAI Techniques for Neural Networks

Given the widespread adoption of deep learning models, there is significant interest in understanding their prediction processes. In particular, visualization-based XAI methods have gained popularity due to their ability to produce intuitive and meaningful results and be applied to explain various deep Convolutional Neural Networks (CNNs). One genre is localization-based explanations, namely attribution heatmaps, which highlight image regions mostly contributing to a specified class prediction, providing class-discriminative localization to support model interpretation. Class Activation Maps (CAM) [48] is a pioneering method, but it requires a specific network architecture, namely the global average pooling layer, to generate visualizations. GradCAM [37] addresses this limitation by using the network’s gradients to compute the model’s attributions. In our work, we utilize GradCAM attribution heatmaps in two ways: firstly, we use them to explain model predictions on single images. Secondly, we interpolate the attributions into weight matrices at the latent space to obtain attribution-weighted feature vectors, which are used to obtain and visualize data slices with similar model attribution patterns.

Another popular approach for understanding model behavior is optimization-based visual explanations. Feature Visualization [10, 27] creates images that maximally activate specific neurons, channels, or layers of a neural network, which focuses on understanding the kind of features a model is sensitive to. Another popular method in this group, feature inversion [24] seeks to understand the information encapsulated in a group of feature representations. Specifically, Feature Inversion generates artificial images that visually elucidate the shared significant patterns of those latent vectors from the model’s perspective.

3 AttributionScanner

In this section, we introduce *AttributionScanner*, a novel approach toward metadata-agnostic ML model validation leveraging slice-level analysis. To foster a thorough understanding of our system, we first outline the requirements that shaped our design choices. Then, we delve into the visual components of *AttributionScanner* that enable interpretable model validation. We then detail our slice computation and summarization methodology, which allows us to generate data slices with consistent model attribution devoid of any additional meta information. Finally, we show how the insights from our system can be used to enhance the model.

3.1 Design Requirements

Slice-Finding has garnered increased attention due to its potential in facilitating a thorough ML model evaluation. However, this task is particularly challenging in the realm of vision models considering the inherent unstructured nature of the data. A pivotal shortcoming we observed in existing approaches is their dependency on metadata or language-vision models to generate meaningful data slices. The acquisition of additional meta-information, when unavailable, entails labor-intensive annotations, demanding substantial human effort and financial investment. Additionally, the language-vision models are commonly trained on general-purpose datasets, potentially leading to inaccurate or biased evaluations in specific domains. Stemming from these observations, we delineated the subsequent requirements for a system capable of conducting metadata-free, slice-driven model validation:

- [R1] *Metadata- and model-less.* Our method should yield meaningful data slices, i.e., slices that share a significant attribution pattern, without access to any meta-information or vision-language models.
- [R2] *Interpretability.* The system should support slice-level and instance-level interpretations. Diverging from prior metadata-free slice-finding approaches for vision tasks, our system should explain data slices by visualizing their shared attributions and also support attribution inspection of individual instances.

[R3] *Slice Overview.* Manual inspection of each slice’s individual images is impractical, especially with a high volume of data. To address this issue, our system should provide a visual summary of the data slices, depicting each data slice’s key features and attributions.

[R4] *Actionable insights.* The system should provide actionable insights by enabling the annotation of data slices. This allows further expert engagement, such as re-labeling or model re-training, to enhance model performance.

3.2 System Workflow

AttributionScanner is a human-in-the-loop system, taking as input an image dataset and a trained CNN for image classification, and yielding interpretable data slices for expert-driven vision model validation [R1].

A workflow of our approach is presented in Fig. 2, where we build upon XAI techniques, namely GradCAM [37] and Feature Inversion [27], to foster explainable slice-finding [R2]. The first “explainable data slice-finding” phase interpolates model attributions from GradCAM into latent space to craft attribution-weighted feature vectors, thereby forming an attribution representation space. We cluster such vectors to generate slices maintaining consistent attributions (Sec. 3.4). Although the produced slices share similar attributions, they still demand significant human effort to identify their patterns. To streamline slice exploration and issue detection, the “slice summarization and annotation” phase introduces *Data Slice Mosaic*, which visually elucidates each slice’s dominant attributions [R3], synchronized with instance-level heatmaps for problem detection and insight verification [R2]. Upon user annotation of an issue like “spurious correlations” [R4], our Spuriousness Propagation method automatically estimates spuriousness scores to help users uncover other hidden model biases. Afterward, our workflow enables the mitigation of detected issues in data or model [R4], corresponding to the “slice error mitigation” phase.

The rest of this section delineates our interface for data slicing-based model validation, explains our presented data slicing and summarization approach, discusses design considerations, and demonstrates how the model can be fine-tuned to rectify detected slice issues.

3.3 System Interface

AttributionScanner is comprised of four main components. Fig. 1 depicts an use case where our system is used to validate a hair color classification model.

The System Menu (Fig. 1 A) provides options for dataset and model version selection, visualization layout configuration, and color encoding choice. Two visualization layouts are available: Combination view or Confusion Matrix view, allowing for an overarching view of data slices or a more detailed inspection segregated by error types [R3]. The color encoding menu offers categorical selections including Slice Name, Slice Accuracy, Slice Confidence, and Spuriousness probability, adaptable to user preferences.

The Slice Table (Fig. 1 B) presents slice metrics to aid in dataset navigation. Available metrics encompass Accuracy, Confidence, and Spuriousness probability, the latter of which is derived through the Spuriousness Propagation method predicated on user annotation (Sec. 3.5.2). This table facilitates user navigation to intriguing slice patterns, like correct attributions with low accuracy possibly indicative of mislabeled instances. Conversely, high accuracy in a spurious slice may signify the model’s vulnerability to certain correlations [R3] [R4].

Our system’s third component is the *Data Slice Mosaic*, rendering the dominant visual patterns of each slice with respect to the model’s decision [R2][R3], either in a unified form (Fig. 1 C) or segregated by the model’s confusion matrix (Fig. 1 D). The design methodology for this view is detailed in Sec. 3.5.1. Moreover, *Data Slice Mosaic* incorporates visualization of user-specified metrics through the coloration of mosaic boundaries, providing a vital guide in pinpointing problematic slices [R3]. Annotation of a slice is facilitated by a double-click action on a mosaic tile, allowing for effortless insight collection [R4].

The Slice Detail View (Fig. 1 D) showcases image samples of the selected data slice, rendering either images or attribution heatmaps. This view enables an in-depth examination of each slice [R2].

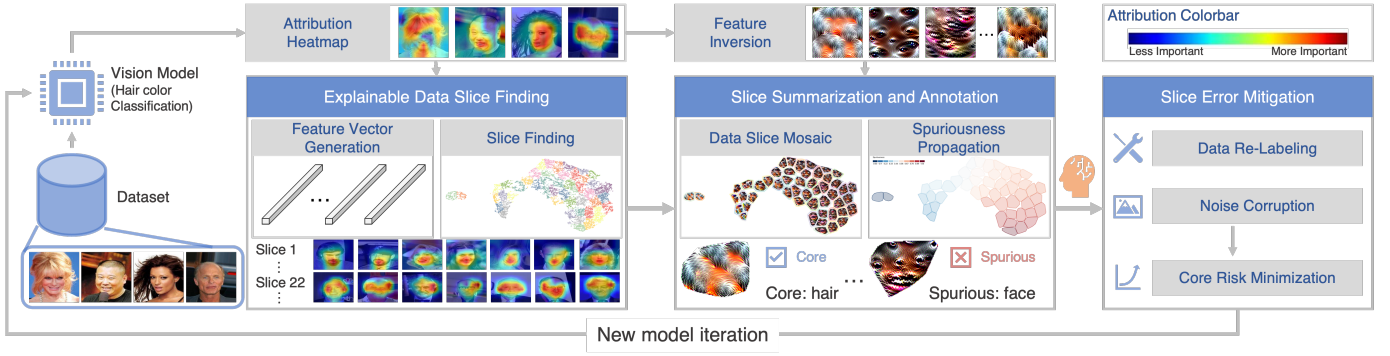


Fig. 2: *AttributionScanner* Workflow involves three phases: *Explainable Data Slice-Finding*, *Slice Summarization and Annotation*, and *Slice Error Mitigation*. The first phase: GradCAM is used to assist the generation of feature vectors and then obtain data slices. The second phase: users can identify and annotate slice error types such as core/spurious correlations and noisy labels with the help of *Data Slice Mosaic* and Spuriousness propagation. The third phase: the annotation and user-verified Spuriousness are used on the ML side to mitigate slice errors, including (1) Data re-labeling if considered necessary, and (2) noise corruption and Core Risk Minimization (CoRM) applied if spurious correlations are detected.

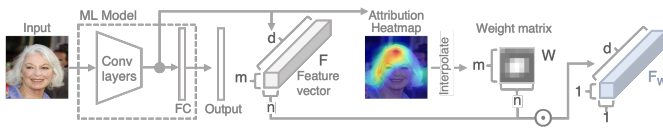


Fig. 3: Attribution-weighted feature vector generation. The image is forwarded through the CNN to extract the feature vector F and generate the attributions heatmap. Then, the attribution mask is linearly interpolated into the latent space to obtain a weight matrix W , which is then utilized to calculate the attribution-weighted feature vector F_W .

3.4 Explainable Data Slice-Finding

In this section, we delineate our Explainable Data Slicing method. Our approach presumes a typical CNN model architecture, comprising a sequence of convolutional layers succeeded by a fully connected (FC) layer, a commonality across most CNN models [15, 37, 38].

The process unfolds in three phases: initially, we create attribution-weighted feature vectors utilizing the interpolated attribution masks in the latent space. Subsequently, we derive an attribution representation space that maintains neighbor consistency in terms of model attributions, enabling us to compute interpretable data slices for metadata-free model validation. Lastly, we employ the Feature Inversion [24] to distill shared visual patterns per slice and visualize these patterns alongside model performance indicators in *Data Slice Mosaic*.

3.4.1 Attribution-Weighted Feature Vector Generation

In this section, we illustrate the process of generating attribution-weighted feature vectors based on attribution heatmaps. It is notable that *AttributionScanner* accommodates interchangeable attribution explanation techniques, such as CAM [48], GradCAM [37], or RISE [33]. Our prototype leverages GradCAM due to its demonstrated efficacy via sanity checks [1] and its prevalent usage for model validation in the ML community [18, 19, 25, 34, 43, 45, 51].

As shown in Fig. 3, an input image is processed by the model to extract the feature vector F , and a back-propagation from the model’s prediction is conducted to obtain the GradCAM attribution masks. While the mask can be depicted as heatmaps for instance-level explanation, we augment it to foster a more comprehensive understanding of the model’s attribution patterns at a macroscopic level. Specifically, we apply linear interpolation to downsample image-sized masks into the latent space, yielding a weight matrix W of dimensions $m \times n$, to compute the weighted average of F . The resulting attribution-weighted feature vector F_W of shape $1 \times 1 \times d$ can be mathematically expressed

$$\text{as: } F_W = \frac{\sum_{i=1, j=1}^{i=m, j=n} F_{ij} W_{ij}}{\sum_{i=1, j=1}^{i=m, j=n} W_{ij}}.$$

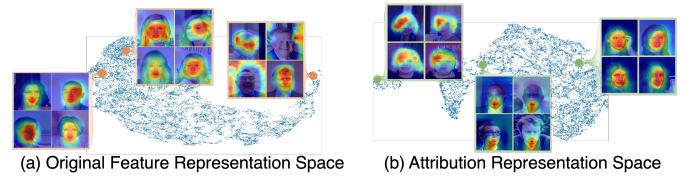


Fig. 4: Comparison of the representation spaces for the hair color classification model. (a) Original feature representation space via UMAP on feature vectors. (b) Attribution representation space via UMAP on attribution-weighted feature vectors. Highlighted images indicate that only (b) maintains neighbor consistency regarding similar model attributions, facilitating interpretable data slice generation.

3.4.2 Data Slice Identification

To derive meaningful data slices exhibiting similar attribution patterns [R1] [R2], we obtain an attribution representation space using the attribution-weighted feature vectors F_W (Sec. 3.4.1). Fig. 4 contrasts the original feature representation space (derived from the original feature vectors) with the attribution representation space (derived from the attribution-weighted feature vectors). For both spaces, we utilize UMAP [26] for dimensionality reduction. By randomly selecting three points and examining the attribution heatmaps of their nearest neighbors in the representation space, we observe, as showcased in Fig. 4, that unlike the original space, the attribution representation space aptly groups instances with coherent attributions. This facilitates the computation of data slices with consistent attribution patterns.

After we extract the attribution-weighted feature vectors, we proceed by clustering the samples with K-Means to obtain data slices. Similarly to DOMINO [11], we apply over-clustering by incrementing the value of K and qualitatively monitoring the model attribution consistency within each slice, until a coherent grouping of samples is attained. This measure helps prevent the omission or overlooking of rare slices, ensuring a comprehensive slice identification.

3.5 Slice Summarization and Annotation

3.5.1 Data Slice Mosaic

Although we have derived slices with consistent model attributions, validating the attribution correctness of each slice necessitates individual inspection of their encompassed data samples. This process is labor-intensive and time-consuming, posing the risk of overlooking critical issues. Therefore, a more efficient method to encapsulate the essence of each data slice is imperative. In response, we introduce *Data Slice Mosaic*, a novel visualization technique that elevates Feature Inversion to visually summarize data slices in a mosaic depiction. We present the pipeline in Fig. 5. First, after the execution of Data Slice-Finding

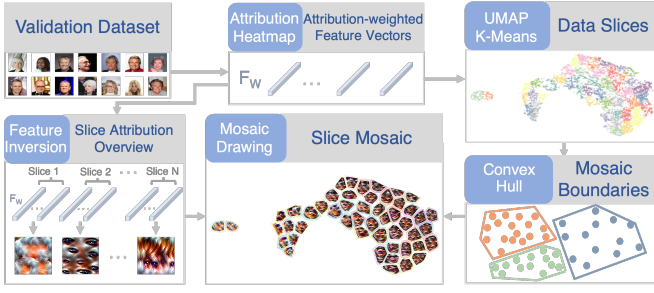


Fig. 5: Pipeline for generating *Data Slice Mosaic*. We first acquire attribution-weighted feature vectors, followed by computing data slices within the attribution representation space (refer to Fig. 3 and Sec. 3.4). Utilizing the Convex Hull of each slice in the 2D space, we create the *Data Slice Mosaic* by producing Feature Inversion for every slice, elucidating their shared visual patterns. This visualization enables users to explore interrelationships among data slices and pinpoint key visual patterns that distinguish them.

(Sec. 3.4), we compute the convex hull of each slice based on the projected points in the 2D space. We then distill each slice’s predominant visual patterns via Feature Inversion, integrating the shape constraint of the convex hull. The final landscape featuring slices’ attribution summaries is presented as *Data Slice Mosaic*.

Slice Summary. A pivotal step in generating *Data Slice Mosaic* involves visually summarizing the significant pattern inherent in each slice. As discussed in Sec. 2.2, Feature Inversion visualizes common information across a group of feature representations. Inspired by Activation Atlas [6], which employs this technique to summarize spatial feature vectors to understand the key patterns learned by the model, we utilize Feature Inversion on the attribution-weighted feature vectors of each data slice to visualize their shared model attributions. Formally, Feature Inversion is defined by:

$$x^* = \arg \max_{x \in \mathbb{R}^{W \times H \times C}} (\ell(\phi(x), \phi_0) + \lambda R(x)),$$

where $\phi : \mathbb{R}^{W \times H \times C} \rightarrow \mathbb{R}^d$ is the representation function; ϕ_0 is a target feature activation; $\ell(\cdot)$ is the loss function, and $R(x)$ is a regularization term [24]. In our scenario, we designate the optimization target, ϕ_0 , to be the average of attribution-weighted feature vectors within a data slice, and assign the representation function to the model’s convolutional modules. We reconstruct a randomly initialized image x^* to minimize the loss function, thereby creating an image that best portrays shared attribution patterns within a data slice from the model’s perspective.

Mosaic Boundary Generation. The main purpose of this stage is to devise a clear layout enabling effortless exploration of diverse attribution patterns across slices. Merely obtaining and displaying the Feature Inversion results over the projected cluster centroids leads to overlapped visualizations, hindering effective user exploration. We design a mosaic layout, optimized for space-efficiency in information representation. Specifically, we compute convex hull [4] of each slice in the attribution representation space, yielding a convex hull for every slice with no overlap amongst them.

Mosaic drawing. Given that the convolutional modules take rectangular-shaped input, the original Feature Inversion algorithm solely generates rectangular visualizations. To preserve equivalent visualization in a mosaic form, we use our generated mosaic boundary as a constraint for optimization. Namely, we define the shape of x^* as the minimal rectangle encompassing the corresponding convex hull, and in each iteration, we zero out pixels outside the hull, compelling the optimization to concentrate on the interior pixels. After rendering all feature visualizations, they are exhibited at their respective positions within the *Data Slice Mosaic*.

3.5.2 Slice Annotation and Spuriousness Propagation

The *Data Slice Mosaic* is a powerful tool that facilitates rapid comprehension of slice contents, supporting the identification of errors

Table 1: System Design Considerations.

Design Components				System Capabilities			
Slice Table	Slice Detail View	Scatter Plot	Data Slice Mosaic	Slice Performance	Slice Attribution	Instance Performance	Instance Attribution
✓	✓			✓			✓
✓	✓	✓		✓		✓	✓
✓	✓		✓	✓	✓	✓	✓

in data or models. A prevalent error in ML models, highly visible through *Data Slice Mosaic*, is “spurious correlation”, where a model erroneously utilizes irrelevant image features for classification. For instance, in hair color classification, a model should leverage hair features, termed as “correct/core correlation”, while the use of other features (e.g., background or facial attributes) denotes “spurious correlation.”

Such spurious correlations, regardless of model accuracy, pose substantial challenges including poor generalization in production [39] and AI fairness issues [23]. To effectively detect these, we introduce a metric termed Spuriousness probabilities, ranging from 0 to 1, indicative of the likelihood of spurious correlation existence. We employ the label propagation method called Label Spreading [50], implemented in *scikit-learn* [32], which indicates potential spuriousness of unannotated slices. Specifically, the minimal input requirement from users is one slice annotation of “core” (Spuriousness=0) or “spurious” (Spuriousness=1), and then *AttributionScanner* will propagate this information to create a Spuriousness probability for the rest slices.

The Spuriousness probabilities obtained through the *Data Slice Mosaic* visualization tool offer two benefits. First, they streamline slice exploration by highlighting potential spurious correlations, aiding users in identifying and assessing problematic slices. Second, after users’ verification, these probabilities inform the model-side strategies to mitigate identified issues (Sec. 3.7).

3.6 System Design Considerations

In designing *AttributionScanner*, various combinations of system components have been contemplated to ensure optimal system capabilities. The deliberation is outlined in Table 1, where diverse system component configurations are evaluated against crucial system capabilities. To fulfill our design requirements discussed in Sec. 3.1, our system should be capable of providing: (1) slice performance indicator[R3], (2) slice attribution overview[R2][R3], (3) instance performance indicator[R2], and (4) instance attribution inspection[R2][R4]. The notions in “design components” are consistent with Fig. 1.

The initial configuration, “Slice Table & Slice Detail View,” is capable of presenting slice performance indicators and instance attributions. However, the numerical matrices of performance indicators are not sufficient in guiding users to uncover hidden model issues, such as spurious correlations that can happen regardless of high or low performance. A subsequent iteration included a scatter plot showing the attribution representation space. This configuration enables the system’s instance performance indicator capability but still misses the slice attribution overview. To the best of our knowledge, there exist few approaches that visually elucidate potential model spuriousness in scale, where our third configuration fulfills this gap — “Slice Table & Slice Detail View & *Data Slice Mosaic*,” which comprehensively satisfies all the essential system capabilities.

Data Slice Mosaic, alongside the Slice Table and Slice Detail View, significantly enriched the system’s ability to provide granular insight into both slice and instance-level attributions and performance indicators. The coordinated Slice Table and *Data Slice Mosaic* can guide users to pinpoint initially hidden model issues, and the Slice Detail View is a further step for users to verify their insights. This robust configuration underscores our meticulous design process in assuring that *AttributionScanner* is not only capable of furnishing critical insights but does so in a manner that is intuitive and user-friendly.

The tabulated design considerations and the ensuing choice of system component configuration aim at maximizing the system’s utility and user-centric functionality. With our finalized configuration (the last row

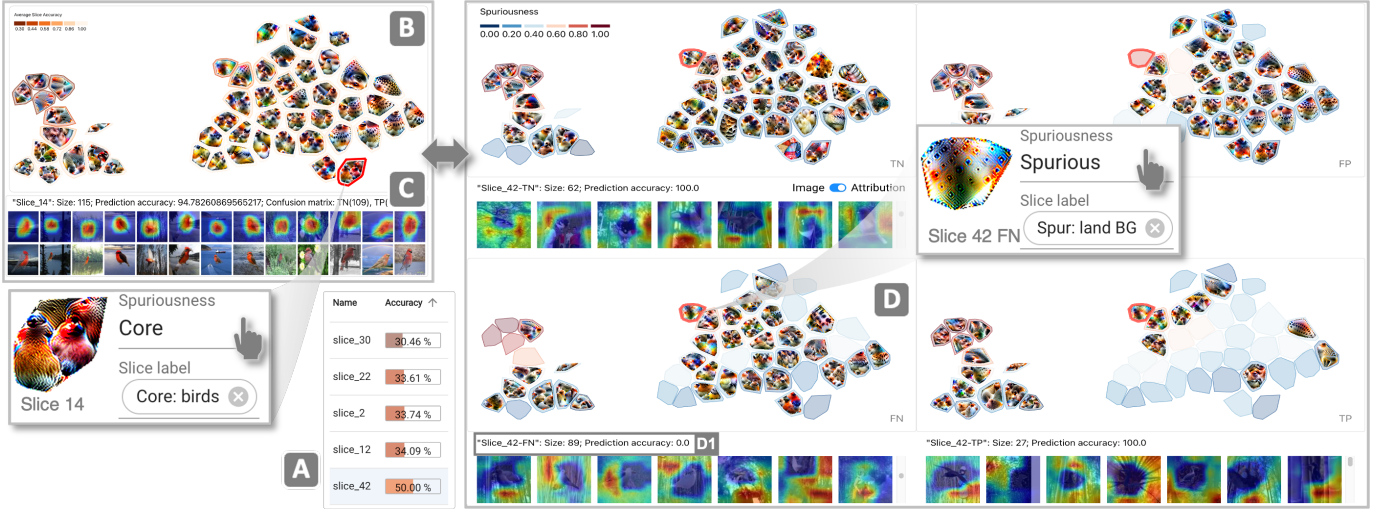


Fig. 6: *AttributionScanner* applied to the validation of a bird category classification model trained on the Waterbirds image dataset [42]. The user finds the correct model behavior (bird patterns) corresponding to a well-performed *Slice 14* and annotates it as “core: birds” B and C. By switching the *Data Slice Mosaic* to the confusion matrix view D and investigating the underperformed slices with accuracy sorting A, the user identifies a problematic *Slice 42* that has high false negatives D1, which turns out to use spurious feature of land backgrounds (BG) to predict landbirds.

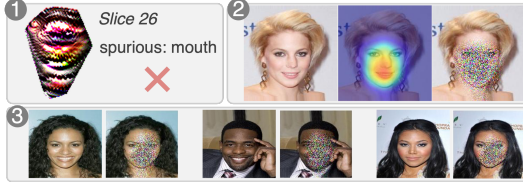


Fig. 7: Example of spurious correlation mitigation with CoRM for a hair color classifier: 1 The data slice summary indicates that this is a problem with a spurious feature: mouth. 2 An example of how the Core Risk Minimization (CoRM) method: Original Image (left), GradCAM activations (middle), noise added to the spurious regions of the image (right) For illustration purposes, the gaussian noise added is exaggerated. 3 More examples with the gaussian noise added to the spurious regions.

of Table 1), users are empowered with sufficient support for problem detection, interpretation, and mitigation in the model validation.

3.7 Slice Error Mitigation

One effective approach to mitigating spurious correlations in ML models is through model re-training, which can improve the model’s robustness against potential bias without changing its architecture. We leverage the Core Risk Minimization (CoRM) method introduced in [39] to reduce the model’s reliance on spurious features. CoRM corrupts non-core image regions with random Gaussian noise and retrain the model using the noise-corrupted data, which has been shown to be effective in mitigating a model’s reliance on spurious features.

To apply CoRM in *AttributionScanner*, we first export slices with high Spuriousness probabilities after users’ annotations, which indicate the presence of undesired correlations. For the images in these slices, the model attribution masks (e.g., GradCAM masks) highlight spurious regions and we utilize such masks to add random Gaussian noise to spurious regions. For a single image, this process can be represented by $\mathbf{x}' = \mathbf{x} + \mathbf{m} \odot \mathbf{z}$, where \mathbf{x} is the input image, \mathbf{m} is the attribution mask, and \mathbf{z} is the generated Gaussian noise matrix. All these three variables are of the same size as the input image, and \odot denotes the Hadamard product. Fig. 7 shows some examples of this operation, with exaggerated noise for presentation purposes. After replacing the original data with these noisy-corrupted slices, we retrain the model and evaluate whether spurious correlation has been reduced. In Sec. 5, we explain the evaluation metrics we use to quantify the effectiveness

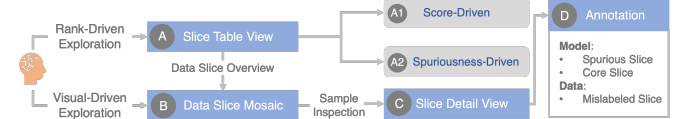


Fig. 8: Usage patterns for *AttributionScanner*, derived from our case studies. The analysis can start with a rank-driven exploration A (ranking the slices by score (e.g., model accuracy) A1 or Spuriousness A2), or a visual-driven exploration B. After inspecting the slice summary in the *Data Slice Mosaic* B, they can inspect individual samples in the *Slice Detail View* C. Finally, they can annotate their insights D.

of *AttributionScanner* in mitigating spurious correlations.

4 CASE STUDIES

In this section, we present two case studies with publicly available vision datasets to benchmark and evaluate the capabilities of *AttributionScanner*. The primary objective of these case studies is to demonstrate how *AttributionScanner* empowers ML experts and practitioners to detect, evaluate, and interpret potential issues in vision models. Fig. 8 illustrates common usage patterns of our system: users can begin the analysis with either a rank-driven evaluation A or a visual-driven evaluation B. Once a slice of interest is identified, users can delve deeper into individual samples in the *Slice Detail View* C. Finally, the user can annotate the data slices and continue their analysis D.

4.1 Hair Color Classifier Validation - Finding Edge Cases

• Overview.

This case study involves the Large-scale CelebFaces Attributes (CelebA) dataset [22] with 202,599 number of face images. The label of each image is one of {not gray hair, gray hair}, refer to labels {0, 1}, respectively. With the train, validation, and test splits of (8 : 1 : 1), we adopt transfer learning to train a ResNet50 [15] binary image classifier. After iteratively fine-tuning hyper-parameters, we obtain a model with 98.03% classification accuracy. The ML experts would then explain and troubleshoot this hair color classifier with *AttributionScanner* based on these settings: $n_neighbors = 5$, $min_dist = 0.01$, and $n_components = 2$ for the UMAP algorithm, and $n_clusters = 50$ for K-Means.

• Does the model behave correctly on well-performing slices?

One basic expected behavior for a hair color classification model is to catch hair features. At first glance of the *Data Slice Mosaic*

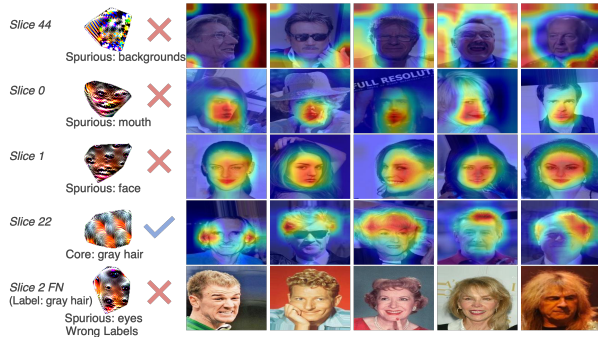


Fig. 9: Examples of the detected issues when ML experts validate a hair color classifier trained on the CelebA dataset, where experts discover slices corresponding to the model’s core/spurious correlations and wrong labels existing in the dataset.

(Fig. 1 C), ML experts notice *slice_22* and *slice_5* on the left, which lie separately with others on the *Data Slice Mosaic*. Their mosaic visualizations indicate gray hair patterns, which means the model uses the correct features, i.e., core features. By verifying the corresponding attribution heatmaps (Fig. 1 D), they confirm the correctness of this insight and annotate both slices as *core feature* with description *Core: gray hair*. Upon experts saving the annotation, *AttributionScanner* automatically propagates the annotation and provides a Spuriousness probability of each slice. With this guidance, the experts observe many slices lying on the right of *Data Slice Mosaic* have higher Spuriousness probabilities (Fig. 1 C B). Their mosaic visualizations do not show any hair patterns, leading to valid doubts that the model does not behave correctly on such slices. Besides, they also notice that the model has correct predictions on these slices (with 100% prediction accuracy). This makes them worry that the model is largely biased by spurious features. Through investigation, they find the model mistakenly utilizes mouth and eyes to predict hair color for those top-performed slices, such as *slice_0*, *slice_1*, and *slice_2* (Fig. 9).

• Why slices underperform?

The experts are also eager to investigate the underperformed slices. By sorting the Slice Table (Fig. 1 B) by ascending order of accuracy, they notice the model only achieves 72.41% accuracy on *slice_44* and find that the slice’s mosaic visualization only shows non-meaningful colorful patterns without any recognizable content. After checking the attribution heatmaps, they find that the model mistakenly uses image backgrounds to make hair color predictions (Fig. 9). This spurious correlation issue stands out, and they annotate this slice as “spurious” with the description “Spurious: backgrounds”. Similar issues also occur in its neighborhood slices via *Data Slice Mosaic*, and *AttributionScanner* automatically propagates them with higher Spuriousness.

• What underlying factors contribute to unexpected behaviors?

ML experts are interested in understanding why such unexpected model behaviors happen. By sorting the Slice Table by descending order of *Spuriousness*, they get a list of slices with high Spuriousness possibilities. They switch *Data Slice Mosaic* into the confusion matrix form (Fig. 1 E) to study further details. By clicking on the name of “*slice_35*”, they highlight this slice on the four sub-views and inspect the provided explanations, where they notice that images that lie in the “FN” group of this slice have wrong labels — they should be labeled as “not gray hair” rather than “gray hair”. They mark this issue as wrong labels and wonder whether this situation is common. By investigating its neighborhood slices on *Data Slice Mosaic*, they find and mark another slice with wrong labels through a few clicks, *slice_2_FN*.

• Insights summary.

Fig. 9 presents examples of the detected issues with the current model, which include wrong attributions in underperforming slices, model biases in well-performing slices, and noisy label issues. Through the aforementioned procedure in this case study, we demonstrate how *AttributionScanner* supports users to uncover and interpret potential

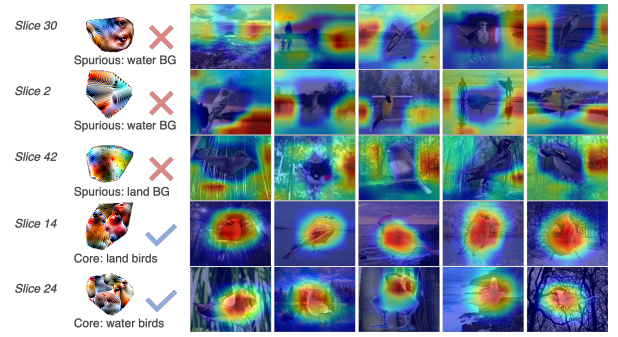


Fig. 10: Example of the detected issues when ML experts validate a bird category classifier trained on the Waterbirds dataset, where *AttributionScanner* identifies problematic slices with spurious background (BG) features: Slices 30 and 2 with water BG used for waterbird prediction, and Slice 42 with land BG used for landbird.

model issues with visual summaries and other guidance. Based on annotations from ML experts, we employ the CoRM framework to mitigate the detected errors, which will be evaluated in Sec. 5.

4.2 Bird Category Classifier Validation - Detecting Bias

• Overview.

To study whether *AttributionScanner* can help ML experts and practitioners find the potential biases and discrimination of models, we design this case study with a biased dataset called Waterbirds [36], which is constructed by cropping out birds from images in the Caltech-UCSD Birds-200-2011 (CUB) dataset [42] and transferring them onto backgrounds from the Places dataset [49]. For each image, the label belongs to one of {*waterbird*, *landbird*}, and the image background belongs to one of {*water background*, *land background*}. The training set is skewed by placing 95% of waterbirds (landbirds) against a water (land) background and the remaining 5% against a land (water) background. Following the same data splitting as [36], the train, validation, and test sets include 4795, 1199, and 5794 images, respectively. After training and fine-tuning hyper-parameters, the waterbirds/landbirds classification model achieves 85.74% classification accuracy. In the data slice finding, we set $n_neighbors = 20$, $min_dist = 0.05$, and $n_components = 2$ for the UMAP algorithm, and $n_clusters = 50$ for K-Means.

While in this study, ML experts are aware that the model is likely biased by backgrounds — using water (land) background to classify waterbirds (landbirds). However, such priori knowledge is hard to establish in real-world applications because of the scarcity of additional well-labeled metadata. And hence the experts assume such information is unknown and want to validate whether *AttributionScanner* can make the potential model biases stand out by only utilizing the original images and the trained model.

• Does the model exhibit bias?

To answer this key question, the experts start by investigating the underperformed slices. From the Slice Table (Fig. 6 A), they sort the listed slices by ascending order of accuracy and select the worst-performed *slice_30*. The coordinated information provided by Feature Inversion and model attribution heatmaps highlights a spurious correlation problem — the model uses water backgrounds to classify birds (Fig. 10). The experts annotate this slice as “spurious”, and *AttributionScanner* automatically propagates this annotation. They verify the propagation correctness on neighborhood slices and annotate *slice_2* as “spurious” with “water backgrounds” (Fig. 10). Moreover, the experts identify an underperformed *slice_42* that is not clustered with the current ones and is given a high Spuriousness possibility. They investigate this slice and verify that the model utilizes “Spurious feature: land backgrounds”, to predict bird classes in this slice. Through the *Data Slice Mosaic* in the confusion matrix form (Fig. 6 D), they find such spurious correlations result in many false negatives (Fig. 6 D1), where the model uses land backgrounds to mistakenly predict many “waterbirds” as “landbirds”.

Table 2: Quantitative evaluation of the overall performance and reliance on spurious features for the hair color classification models trained on the original CelebA dataset and the *AttributionScanner*(AS)-improved CelebA dataset. Performance is evaluated with the validation set.

Training Procedure	Clean Acc (↑)	Core Acc (↑)	Spurious Acc (↓)	RCS (↑)
Baseline	98.02688	97.21170	97.61917	0.067720
AS (Annotation)	98.02688	98.02185	96.92958	0.216351
AS (Propagation)	98.08225	98.16278	96.01852	0.368512

• Is the detected bias prevalent across all slices? Why or why not?

ML experts are interested in determining whether the detected bias is pervasive throughout the dataset. By analyzing slices that are distant from the annotated ones in the *Data Slice Mosaic* and are assigned with low Spuriousness possibilities, they discovered that the farthest neighbors, namely *slice_24* and *slice_14*, correspond to core features. This suggests that the model can correctly capture bird regions in these slices (Fig. 6 B C), which raises a follow-up “why” question. To understand in what circumstances when the model fails. They browse the original images from *slice_42* (spurious feature) and *slice_14* (core feature), respectively, as shown in Fig. 6 D and E. They find *slice_42* has very similar land backgrounds and very different birds, while on the other hand, the birds’ appearance of *slice_14* (core feature) is very consistent. This finding explains why this biased model can still capture the core features from *slice_14* — greater similarities of core features in the representation space leads to greater robustness against spurious correlations. Such insights are helpful in improving model robustness and have been further studied by ML experts [46].

• Insights summary.

A summary of insights obtained from this case study is provided in Fig. 10, where ML experts validate the existence of model biases and extract slices corresponding to different biases. In the following Sec. 5, we evaluate whether *AttributionScanner* can mitigate model errors by incorporating human feedback.

5 EVALUATION

In this section, we conduct both quantitative and qualitative evaluations to validate whether *AttributionScanner* can indeed leverage human insights to enhance vision models’ performance while reducing their reliance on spurious features.

5.1 Quantitative Evaluation

The quantitative evaluation involves four matrices introduced in [39], including clean accuracy, core accuracy, spurious accuracy, and relative core sensitivity (RCS). We revisit their definitions as follows:

- **Clean Accuracy.** The model accuracy calculated on the original dataset, where larger values are indicative of better overall accuracy.
- **Core Accuracy $acc^{(C)}$.** The model accuracy calculated when spurious regions are added with Gaussian noise, where larger values are indicative of the model’s more reliance on core regions.
- **Spurious Accuracy $acc^{(S)}$.** The model accuracy calculated when core regions are added with Gaussian noise, where larger values are indicative of the model’s more reliance on spurious regions.
- **RCS.** This matrix quantifies the model’s reliance on core features while controlling for general noise robustness. It is defined as the ratio of the absolute gap between core and spurious accuracy, and the total possible gap for any model between core and spurious accuracy. Represented as $RCS = \frac{acc^{(C)} - acc^{(S)}}{2 \times \min(\alpha, 1 - \alpha)}$, where $\alpha = \frac{acc^{(C)} + acc^{(S)}}{2}$. RCS ranges from 0 to 1, a higher value indicative of better model performance.

In the two case studies discussed in Sec. 4, ML experts annotated five spurious slices in the CelebA dataset, {*slice_0*, *slice_1*, *slice_2*, *slice_44*, *slice_26*}, and six spurious slices in the Waterbirds dataset, {*slice_30*, *slice_2*, *slice_22*, *slice_12*, *slice_42*, *slice_9*}, respectively. For each case study, *AttributionScanner* automatically ran the Label Propagation algorithm and exported both the users’ annotation records and the propagated Spuriousness for further investigation.

Table 3: Quantitative evaluation of the overall performance and reliance on spurious features for the bird category classification models trained on the original Waterbirds dataset and the *AttributionScanner*(AS)-improved Waterbirds dataset. Performance is evaluated with the validation set.

Training Procedure	Clean Acc (↑)	Core Acc (↑)	Spurious Acc (↓)	RCS (↑)
Baseline	85.73812	82.98582	82.82901	0.004878
AS (Annotation)	89.57465	86.40534	79.81651	0.195062
AS (Propagation)	90.40867	87.40617	77.89825	0.274038

To thoroughly evaluate our introduced method, we validate three models for each case. The models marked as “baseline” are the original trained models obtained at the beginning of each case study. The models marked as “*AttributionScanner*” are re-trained using the CoRM method after adding noise to “spurious” slices according to results exported from *AttributionScanner*. In particular, “Annotation” indicates that only user-annotated spurious slices were corrupted with noise, while “Propagation” indicates that propagated Spuriousness is used to identify spurious slices to be added with noise.

Table 2 and Table 3 present the quantitative evaluation results for the two case studies, respectively. Our presented *AttributionScanner* can significantly improve the vision model’s overall performance with reduced spurious correlations. Furthermore, our Label Propagation largely reduces human effort by automating the annotation process, and achieves the best performance in this quantified evaluation. Overall, our results demonstrate that *AttributionScanner* is an effective approach for mitigating spurious correlations in machine learning models, and the Label Propagation algorithm is a valuable tool for automating the annotation process.

5.2 Qualitative Evaluation

Results in Sec. 5.1 highlight the best performance of *AttributionScanner* equipped with Label Propagation in mitigating spurious correlations. For further evaluation, we visually compare models’ attributions via GradCAM in Fig. 11. Refer to Sec. 4.1, the hair color classifier originally has spurious correlations dominant in {*slice_44*, *slice_0*, and *slice_1*}, where the model uses image backgrounds, mouth, or eyes to predict hair color, respectively. With the help of *AttributionScanner*, the model’s misattribution is successfully fixed, directing focus towards the correct hair regions (refer to Fig. 11(a)). As for the bird category classification model, it originally focuses on spurious features, water/land backgrounds, to decide whether there are water/land birds on the input image {*slice_30*, *slice_2*, and *slice_42*} (refer to Sec. 4.1). In Fig. 11(b), we can observe that *AttributionScanner* mitigates these issues by helping the model to focus on the core bird features.

5.3 Experts Feedback

We conduct two case studies (see Sec. 4.1 and Sec. 4.2) with five ML experts to evaluate *AttributionScanner*. They are not co-authors of this paper and had not previously seen *AttributionScanner*. Three of them possessed over five years of experience in ML, one had between three to five years of experience, and one had between one to three years of experience. All five experts need to conduct model validation in their research. Our findings are drawn from their comments during the study, as they follow the “think-aloud” protocol, and their feedback gathered through exit discussion and questionnaire.

Summary of Likert-Type Questions. The exit questionnaire includes eight Likert-type questions on a five-point scale. The feedback, shown in Fig. 12, reflects a positive overall impression. Notably, four experts strongly agreed that our system helps them in validating models. Four agreed or strongly agreed that our system is user-friendly and understandable. All experts expressed strong confidence in the insights provided and showed interest in employing our system in the future. Given that Feature Inversion results (FI) are artificial images that might be hard to grasp initially, we included questions to evaluate this design. Three experts strongly agreed and one expert agreed that FI is helpful. While the claim of understanding slice contents solely based on FI was met with disagreement by two experts, all experts expressed agreement

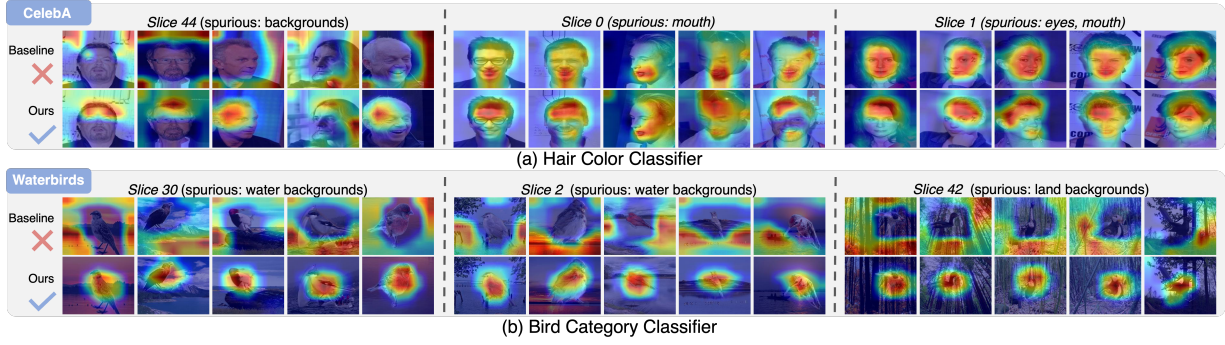


Fig. 11: Qualitative evaluation with the pixel attribution from GradCAM. We visually compare the original classification model and the *AttributionScanner*-improved model for the hair color classification on the CelebA dataset, and the bird category classification on the Waterbirds dataset, respectively. For each sub-figure, the first row refers to the original model, and the second row refers to the improved model. We can observe *AttributionScanner* suppresses the spurious correlations by using the correct features for predictions.

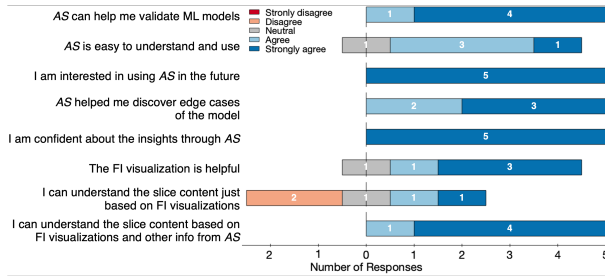


Fig. 12: Expert perception of the system, according to eight Likert-Type Questions using a 5-point scale. (AS = *AttributionScanner*.)

or strong agreement that *AttributionScanner*’s coordination of FI and other views supports a full understanding of slice contents.

Interpretable Model Validation. All experts acknowledged that *AttributionScanner* “effectively helps ML model validation”. They remarked that the complimentary visual summaries and attribution heatmaps help them “easily understand slice issues”. “It’s often hard to figure out what’s going wrong with a model”, one expert said, “This system guides me to find where I should look and explains the issues intuitively.” They commented that they are confident about their insights because our system “highlights slice errors and provides supportive evidence”. Three of them are eager to see what issues *AttributionScanner* could uncover for the models they are currently using.

Data Slice Mosaic. All participants showed particular interest in the *Data Slice Mosaic* and asked about how it was designed in the interview. Two experts pointed out that it is an “impressive and novel” view that enables “an easy detection of slice issues”. One expert commented “This view provides a new angle for me to identify and understand the data/model issues.” All experts quickly adapted Spuriousness propagation and utilized the Spuriousness matrix to speed up their annotation. Specifically, three experts felt that the Spuriousness propagation is “surprisingly helpful” and “really saved my effort”.

Improvements. The experts also suggested some improvements related to our user interface. They thought the Feature Inversion result was not easy to understand at first glance. They mentioned “adding some additional information about each mosaic tile would help.” Besides, one expert suggested we directly show predictions and labels via text in each confusion matrix panel. “It would be better if you show ‘label: waterbirds; prediction: landbirds’ rather than ‘TN’”.

6 DISCUSSION AND FUTURE WORK

Potential risks introduced by XAI techniques.

In this work, we leverage state-of-the-art XAI techniques including GradCAM and Feature Inversion, where the first is one of the most

widely-adopted attribution-based explanations for neural networks [2, 21, 28, 34] and the second is an advanced technique to visualize what a model is looking for [6, 16, 41]. However, there has been continuing discussion on the reliability and trustworthiness of XAI techniques [1, 12], indicating the potential risks of using them. Even though both of them have been proven to retain a level of correctness through validations such as saliency checks [1], we are aware of such risks and involve human auditions in our workflow to alleviate them. In the future, we plan to design more trustworthy model explanations by reasoning about the causality relationships in model decisions [14, 31], and continue to involve human-in-the-loop to mitigate pitfalls in AI-automated tools.

Propagation approaches for the hypothetical spuriousness.

We adopt the Label Propagation method [50] to automatically spread the slices’ spurious annotations from users to other slices as discussed in Sec. 3.5.2. This is under the assumption that the distance between the slices corresponding to spurious correlations (e.g., water backgrounds) and the slices corresponding to core correlations (e.g., birds) is large. However, such assumptions can be invalid in other scenarios. For example, an image classification model trained on ImageNet [8] includes various different classes such as “husky dog” and “king penguin”. It is likely that two slices far away from each other are both corresponding to the core correlations. To address this, we plan to incorporate class similarities to the Label Propagation matrix to improve the precision of the generated hypothetical Spuriousness.

Better guidance in data slice finding.

We include the model’s performance indicators such as the classification accuracy and the average prediction confidence, as well as the Spuriousness probabilities in the Slice Table of our system to guide users to find interesting slices (refer to Fig. 1 B). Although the current guidance is proven to be effective in assisting users to detect slice issues, we plan to make further improvements. We aim to introduce new metrics calculated based on the model’s performance, the slice pattern similarity, and the Spuriousness. By doing this, we will provide more informed guidance to our users by leveraging human and model’s knowledge simultaneously, further improving the effectiveness of our model validation workflow.

7 CONCLUSION

In this work, we present *AttributionScanner*, a novel human-in-the-loop model validation system empowered by metadata-free Data Slice-Finding and XAI techniques, which can support effective detection, explanation, and mitigation of potential errors and biases in vision models. To achieve this, we first present a metadata-free data-slicing method by using attribution-weighted features to group image data into interpretable slices. Also, we invent a novel visual summarization method, *Data Slice Mosaic*, which visually presents the shared significant patterns of each slice attributing to model’s decision. This way, *AttributionScanner* is able to provide explainable data slices that reveal

critical model problems, such as spurious correlations and mislabeled data. We also demonstrate the effectiveness of this work in performance improvement and bias mitigation through both quantitative and qualitative evaluations. To sum up, without additional meta-information, multi-modal model, or other background information, *AttributionScanner* enables an effective model validation and error mitigation workflow to alleviate underlying issues in ML models. We hope this work can inspire future research in human-AI teaming to improve AI trustworthiness and accountability.

REFERENCES

- [1] J. Adebayo, J. Gilmer, M. Muelly, I. Goodfellow, M. Hardt, and B. Kim. Sanity checks for saliency maps. *Advances in neural information processing systems*, 31, 2018. 4, 9
- [2] A. B. Arrieta, N. Díaz-Rodríguez, J. Del Ser, A. Bennetot, S. Tabik, A. Barbado, S. García, S. Gil-López, D. Molina, R. Benjamins, et al. Explainable artificial intelligence (xai): Concepts, taxonomies, opportunities and challenges toward responsible ai. *Information fusion*, 58:82–115, 2020. 9
- [3] G. Barash, E. Farchi, I. Jayaraman, O. Raz, R. Tzoref-Brill, and M. Zalmancovich. Bridging the gap between ML solutions and their business requirements using feature interactions. In *Proceedings of the 2019 27th ACM Joint Meeting on European Software Engineering Conference and Symposium on the Foundations of Software Engineering*, pp. 1048–1058, 2019. 2
- [4] C. B. Barber, D. P. Dobkin, and H. Huhdanpaa. The quickhull algorithm for convex hulls. *ACM Transactions on Mathematical Software (TOMS)*, 22(4):469–483, 1996. 5
- [5] Á. A. Cabrera, W. Epperson, F. Hohman, M. Kahng, J. Morgenstern, and D. H. Chau. FairVis: Visual analytics for discovering intersectional bias in machine learning. In *Proceedings of 2019 IEEE Conference on Visual Analytics Science and Technology (VAST)*, pp. 46–56. IEEE, 2019. 2
- [6] S. Carter, Z. Armstrong, L. Schubert, I. Johnson, and C. Olah. Activation atlas. *Distill*, 2019. <https://distill.pub/2019/activation-atlas>. doi: 10.23915/distill.00015 5, 9
- [7] Y. Chung, T. Kraska, N. Polyzotis, K. H. Tae, and S. E. Whang. Slice finder: Automated data slicing for model validation. In *2019 IEEE 35th International Conference on Data Engineering (ICDE)*, pp. 1550–1553. IEEE, 2019. 1, 2
- [8] J. Deng, W. Dong, R. Socher, L.-J. Li, K. Li, and L. Fei-Fei. Imagenet: A large-scale hierarchical image database. In *2009 IEEE conference on computer vision and pattern recognition*, pp. 248–255. Ieee, 2009. 9
- [9] G. d’Eon, J. d’Eon, J. R. Wright, and K. Leyton-Brown. The spotlight: A general method for discovering systematic errors in deep learning models. In *2022 ACM Conference on Fairness, Accountability, and Transparency*, pp. 1962–1981, 2022. 1, 2
- [10] D. Erhan, Y. Bengio, A. Courville, and P. Vincent. Visualizing higher-layer features of a deep network. *University of Montreal*, 1341(3):1, 2009. 3
- [11] S. Eyuboglu, M. Varma, K. K. Saab, J.-B. Delbrouck, C. Lee-Messer, J. Dunnmon, J. Zou, and C. Re. Domino: Discovering systematic errors with cross-modal embeddings. In *International Conference on Learning Representations*, 2022. 1, 2, 4
- [12] A. Ghorbani, A. Abid, and J. Zou. Interpretation of neural networks is fragile. In *Proceedings of the AAAI conference on artificial intelligence*, vol. 33, pp. 3681–3688, 2019. 9
- [13] D. Gunning. Explainable artificial intelligence (xai). *Defense advanced research projects agency (DARPA), nd Web*, 2(2):1, 2017. 1
- [14] J. Y. Halpern and J. Pearl. Causes and explanations: A structural-model approach. part i: Causes. *The British journal for the philosophy of science*, 2020. 9
- [15] K. He, X. Zhang, S. Ren, and J. Sun. Deep residual learning for image recognition. In *Proceedings of the IEEE conference on computer vision and pattern recognition*, pp. 770–778, 2016. 4, 6
- [16] F. Hohman, H. Park, C. Robinson, and D. H. P. Chau. Summit: Scaling deep learning interpretability by visualizing activation and attribution summarizations. *IEEE transactions on visualization and computer graphics*, 26(1):1096–1106, 2019. 9
- [17] M. Kahng, D. Fang, and D. H. Chau. Visual exploration of machine learning results using data cube analysis. In *Proceedings of the Workshop on Human-In-the-Loop Data Analytics*, pp. 1–6, 2016. 2
- [18] A. Krishnakumar, V. Prabhu, S. Sudhakar, and J. Hoffman. Udis: Unsupervised discovery of bias in deep visual recognition models. In *British Machine Vision Conference (BMVC)*, vol. 1, p. 3, 2021. 2, 4
- [19] S. Lee, A. Payani, and D. H. P. Chau. Towards mitigating spurious correlations in image classifiers with simple yes-no feedback. 4
- [20] S. Lee, Z. J. Wang, J. Hoffman, and D. H. P. Chau. Viscuit: Visual auditor for bias in cnn image classifier. In *Proceedings of the IEEE/CVF Conference on Computer Vision and Pattern Recognition*, pp. 21475–21483, 2022. 2
- [21] P. Linardatos, V. Papastefanopoulos, and S. Kotsiantis. Explainable ai: A review of machine learning interpretability methods. *Entropy*, 23(1):18, 2020. 9
- [22] Z. Liu, P. Luo, X. Wang, and X. Tang. Deep learning face attributes in the wild. In *Proceedings of International Conference on Computer Vision (ICCV)*, December 2015. 1, 6
- [23] M. A. Madaio, L. Stark, J. Wortman Vaughan, and H. Wallach. Co-designing checklists to understand organizational challenges and opportunities around fairness in ai. In *Proceedings of the 2020 CHI Conference on Human Factors in Computing Systems*, pp. 1–14, 2020. 5
- [24] A. Mahendran and A. Vedaldi. Understanding deep image representations by inverting them. In *Proceedings of the IEEE conference on computer vision and pattern recognition*, pp. 5188–5196, 2015. 3, 4, 5
- [25] C. Mao, K. Xia, J. Wang, H. Wang, J. Yang, E. Bareinboim, and C. Vondrick. Causal transportability for visual recognition. In *Proceedings of the IEEE/CVF Conference on Computer Vision and Pattern Recognition*, pp. 7521–7531, 2022. 4
- [26] L. McInnes, J. Healy, and J. Melville. Umap: Uniform manifold approximation and projection for dimension reduction. *arXiv preprint arXiv:1802.03426*, 2018. 4
- [27] C. Olah, A. Mordvintsev, and L. Schubert. Feature visualization. *Distill*, 2017. <https://distill.pub/2017/feature-visualization>. doi: 10.23915/distill.00007 2, 3
- [28] T. Ozturk, M. Talo, E. A. Yildirim, U. B. Baloglu, O. Yildirim, and U. R. Acharya. Automated detection of covid-19 cases using deep neural networks with x-ray images. *Computers in biology and medicine*, 121:103792, 2020. 9
- [29] E. Pastor, L. de Alfaro, and E. Baralis. Looking for trouble: Analyzing classifier behavior via pattern divergence. In *Proceedings of the 2021 International Conference on Management of Data*, pp. 1400–1412, 2021. 1, 2
- [30] E. Pastor, A. Gavaganian, E. Baralis, and L. de Alfaro. How divergent is your data? *Proceedings of the VLDB Endowment*, 14(12):2835–2838, 2021. 1, 2
- [31] J. Pearl. *Causality*. Cambridge university press, 2009. 9
- [32] F. Pedregosa, G. Varoquaux, A. Gramfort, V. Michel, B. Thirion, O. Grisel, M. Blondel, P. Prettenhofer, R. Weiss, V. Dubourg, et al. Scikit-learn: Machine learning in python. *the Journal of machine Learning research*, 12:2825–2830, 2011. 5
- [33] V. Petsiuk, A. Das, and K. Saenko. Rise: Randomized input sampling for explanation of black-box models. *arXiv preprint arXiv:1806.07421*, 2018. 2, 4
- [34] L. Rieger, C. Singh, W. Murdoch, and B. Yu. Interpretations are useful: penalizing explanations to align neural networks with prior knowledge. In *International conference on machine learning*, pp. 8116–8126. PMLR, 2020. 1, 4, 9
- [35] S. Sagadeeva and M. Boehm. Sliceline: Fast, linear-algebra-based slice finding for ml model debugging. In *Proceedings of the 2021 International Conference on Management of Data*, pp. 2290–2299, 2021. 1, 2
- [36] S. Sagawa, P. W. Koh, T. B. Hashimoto, and P. Liang. Distributionally robust neural networks for group shifts: On the importance of regularization for worst-case generalization. *arXiv preprint arXiv:1911.08731*, 2019. 2, 7
- [37] R. R. Selvaraju, M. Cogswell, A. Das, R. Vedantam, D. Parikh, and D. Batra. Grad-cam: Visual explanations from deep networks via gradient-based localization. In *Proceedings of the IEEE international conference on computer vision*, pp. 618–626, 2017. 2, 3, 4
- [38] K. Simonyan and A. Zisserman. Very deep convolutional networks for large-scale image recognition. *arXiv preprint arXiv:1409.1556*, 2014. 4
- [39] S. Singla, M. Moayeri, and S. Feizi. Core risk minimization using salient imagenet. *arXiv*, 2022. 5, 6, 8
- [40] N. Sohoni, J. Dunnmon, G. Angus, A. Gu, and C. Ré. No subclass left behind: Fine-grained robustness in coarse-grained classification problems. *Advances in Neural Information Processing Systems*, 33:19339–19352, 2020. 1, 2
- [41] E. Tjoa and C. Guan. A survey on explainable artificial intelligence (xai):

- Toward medical xai. *IEEE transactions on neural networks and learning systems*, 32(11):4793–4813, 2020. [9](#)
- [42] C. Wah, S. Branson, P. Welinder, P. Perona, and S. Belongie. The caltech-ucsd birds-200-2011 dataset. 2011. [6](#), [7](#)
- [43] S. Wu, M. Yuksekgonul, L. Zhang, and J. Zou. Discover and cure: Concept-aware mitigation of spurious correlation. *arXiv preprint arXiv:2305.00650*, 2023. [4](#)
- [44] T. Wu, M. T. Ribeiro, J. Heer, and D. Weld. Errudite: Scalable, reproducible, and testable error analysis. In *Proceedings of the 57th Annual Meeting of the Association for Computational Linguistics*, 2019. [2](#)
- [45] Y. Yang, B. Nushi, H. Palangi, and B. Mirzasoleiman. Mitigating spurious correlations in multi-modal models during fine-tuning. *arXiv preprint arXiv:2304.03916*, 2023. [4](#)
- [46] M. Zhang, N. S. Sohoni, H. R. Zhang, C. Finn, and C. Ré. Correct-n-contrast: A contrastive approach for improving robustness to spurious correlations. *arXiv preprint arXiv:2203.01517*, 2022. [8](#)
- [47] X. Zhang, J. P. Ono, H. Song, L. Gou, K.-L. Ma, and L. Ren. Sliceteller: A data slice-driven approach for machine learning model validation. *IEEE Transactions on Visualization and Computer Graphics*, 29(1):842–852, 2022. [1](#), [2](#)
- [48] B. Zhou, A. Khosla, A. Lapedriza, A. Oliva, and A. Torralba. Learning deep features for discriminative localization. In *Proceedings of the IEEE conference on computer vision and pattern recognition*, pp. 2921–2929, 2016. [2](#), [3](#), [4](#)
- [49] B. Zhou, A. Lapedriza, A. Khosla, A. Oliva, and A. Torralba. Places: A 10 million image database for scene recognition. *IEEE transactions on pattern analysis and machine intelligence*, 40(6):1452–1464, 2017. [7](#)
- [50] D. Zhou, O. Bousquet, T. Lal, J. Weston, and B. Schölkopf. Learning with local and global consistency. *Advances in neural information processing systems*, 16, 2003. [5](#), [9](#)
- [51] J. Zhuang, J. Cai, R. Wang, J. Zhang, and W. Zheng. Care: Class attention to regions of lesion for classification on imbalanced data. In *International Conference on Medical Imaging with Deep Learning*, pp. 588–597. PMLR, 2019. [4](#)